Microphase Separation in Normal and Inverse Tapered Block Copolymers of Polystyrene and Polyisoprene. 1. Phase State

P. Hodrokoukes,[‡] G. Floudas,*[,†] S. Pispas,[‡] and N. Hadjichristidis*[,‡]

Foundation for Research and Technology-Hellas (FO.R.T.H.), Institute of Electronic Structure and Laser, P.O. Box 1527, 711 10 Heraklion Crete, Greece, and Department of Chemistry, University of Athens, Panepistimiopolis, Zografou 15771 Athens, Greece

Received August 24, 2000; Revised Manuscript Received November 8, 2000

ABSTRACT: We have investigated the influence of composition gradients on the microdomain structure and viscoelastic properties of tapered block copolymers by (i) varying the amount of interfacial material and (ii) the block sequence. Normal tapered and inverse tapered triblock copolymers of polystyrene and polyisoperne with a tapered midblock have been synthesized via anionic polymerization with a nearly symmetric composition and compared with the corresponding diblock copolymers. We found that increasing the amount of tapered material within the interface systematically increases the compatibility. Block sequencing is found to be an important factor controlling compatibility. Inverse tapered block copolymers are much more compatible than the corresponding normal tapered block copolymers. Results presented here could be used as a guideline for preparing copolymers with controlled compatibility at the synthesis level.

I. Introduction

Thermoplastic elastomers are composed of a rubber matrix containing inclusions of the hard phase (as spheres or cylinders) and exhibit low modulus, high elongation, and excellent recovery. A typical elastomer is Kraton D1102, a poly(styrene-*b*-butadiene-*b*-styrene) (SBS) triblock copolymer with a molecular weight of 7×10^4 and a butadiene content of about 70%. There has been a challenge to develop more stiff resins with a lower rubber content while preserving the ability of plastic deformation and impact strength. Reduction of the rubber content to about 25% in triblock copolymers leads to higher moduli, but the material becomes brittle instead. A step forward in this direction was made some 40 years ago with a commercial product under the trade name Styrolux. Styrolux KR2691 is a linear SBS copolymer with a molecular weight of 7×10^4 and a butadiene content of only 26%. All other grades of Styrolux, however, are star block copolymers: addition of styrene and butadiene results in a B/S tapered interface,[1] and the mixture consists of short B-rich and long S-rich triblocks coupled with an oligofunctional coupling agent giving on average 4-arm star block copolymers. The morphology of Styrolux was found to be different from the classical phases formed with diblock copolymers with the appearance of wormlike structures.[2]

Recently,[2] a new commercial product with the trade name Styroflex appeared used in extrusion and injection molding, which is suitable for the high-speed processing required in thin films. The product is composed of linear S−S/B−B with a *statistical* S/B sequence at the interface and an overall styrene content of 70%. The advantage of the new product lies in its higher molecular weight (1.4×10^5 vs 7×10^4) at constant viscosity. Despite the higher molecular weight favoring microphase separation, the order-to-disorder transition temperature, T_{ODT}, was found to be at 418 K, which is well below the processing temperature range (443−483 K).[2] The lower T_{ODT} was of key advantage over the conventional SBS block copolymers and facilitated the production of thin films with negligible melt history.

Poly[isoprene-*b*-(isoprene-*co*-styrene)-*b*-styrene] triblock copolymers[3] have also been synthesized with a variable interface thickness by anionic polymerization. The synthesis consisted of a sequential three-step block copolymerization of a pure isoprene block, followed by a *statistical* copolymer of styrene and isoprene and finally a pure styrene block. When the volume fraction of the copolymer was below 60%, a single lamellar morphology was obtained. However, for higher volume fractions of the middle block, three-phase systems were obtained composed of nearly pure PI domains, mixed PS domains, and a third intermediate "phase".

Tapered block copolymers of styrene and isoprene as well as styrene and butadiene have been studied in a series of papers by Hashimoto and co-workers.[4−6] In both cases THF was added as a randomizer during the simultaneous copolymerization of a mixture of the monomers with *s*-BuLi in benzene as the initiator and polymerization solvent, respectively. The presence of THF made the interface more a *statistical* one. The repulsive interaction between the two blocks was found to be reduced due to enhanced mixing. Surprisingly, nonlamellar structures (rodlike) were found even for nearly symmetric compositions.

The structure, thermodynamics, and dynamic properties of tapered block copolymers were also studied with computer simulations.[7] The simulations have shown that the order-to-disorder transition temperature can be controlled over a broad temperature range by changing the composition gradient without any change in the morphology. The dynamic properties of the tapered copolymers were similar to the normal diblocks, albeit shifted continuously along the temperature scale.

These earlier studies have shown a strong influence of the presence of the tapered interface on the mechanical properties and therefore the processability of block copolymers. A study of the influence of the interface on

[†] Institute of Electronic Structure and Laser.
[‡] University of Athens.

10.1021/ma001479i CCC: $20.00
Published on Web 01/03/2001

the structure and viscoelastic properties of tapered block copolymers can best be made by (i) systematically varying the amount of interfacial material and (ii) varying the sequence of appearance of monomers. In the present investigation we have synthesized (i) a triblock copolymer with a tapered middle block, (ii) three triblock copolymers with *inverse* tapered middle blocks, (iii) an all-tapered block copolymer, and (iv) a random copolymer. The monomers were styrene and isoprene, and all copolymers had a nearly symmetric composition. With these systems we can study both the effect of increasing the amount of the interfacial material and the effect of block sequencing. We found that increasing the amount of the tapered middle block in the inverse tapered copolymers systematically increases the compatibility, but the key parameter affecting the compatibility is the block sequencing in the interface with respect to the outer blocks.

II. Experiment

Synthesis. Polymer synthesis was performed in all-glass reactors using break-seals and constrictions. The solvent (benzene), monomers (styrene, isoprene), initiator (*s*-BuLi), and terminating agent (methanol) were purified using well-established high-vacuum methods.[8,9] Potassium alkoxide was generated by the reaction of excess clean potassium metal with vacuum-distilled 2,3-dimethyl-3-pentanol in a specially designed all-glass reactor. A tapered block copolymer (called T5 from now on) was synthesized by taking advantage of the different reactivity ratios of styrene and isoprene when copolymerized in benzene with an anionic polymerization initiator like *s*-BuLi (reactivity ratios:[10] $r(\mathrm{I}) = 14.6$; $r(\mathrm{S}) = 0.05$) according to the following scheme:

$$s\text{-BuLi} + \mathrm{S} + \mathrm{I} \rightarrow \mathrm{P(S{-}I)_t^-\,Li^+}$$

$$\mathrm{P(S{-}I)_t^-Li^+} + \mathrm{MeOH} \rightarrow \mathrm{P(S{-}I)_t}$$

Because of the marked difference in the reactivity ratios, if a mixture of S and I is added in a *s*-BuLi solution in benzene, isoprene is polymerized first until its concentration becomes relatively low. As isoprene becomes depleted, styrene is incorporated in the polymer chain progressively at higher amounts, until it is the only monomer left in the reaction mixture and finally a pure PS block is formed. In general, however, four reactivity ratios are needed (I−S, S−I, S−S, and I−I) for a more complete description of the polymerization reactions.

A triblock copolymer with a tapered middle block (TMB) (called T4) was prepared next. The synthesis started with the addition of isoprene to *s*-BuLi, followed by addition of a mixture of the two monomers (S and I in a 50:50 weight ratio) to the living PI chain and finally addition of styrene. The following scheme is used for the synthesis of T4:

$$\mathrm{I} + s\text{-BuLi} \rightarrow \mathrm{PI^-Li^+}$$

$$\mathrm{PI^-Li^+} + \mathrm{S} + \mathrm{I} \rightarrow \mathrm{PI{-}P(S{-}I)_t^-\,Li^+}$$

$$\mathrm{PI{-}P(S{-}I)_t^-Li^+} + \mathrm{S} \rightarrow \mathrm{PI{-}P(S{-}I)_t{-}PS^-\,Li^+}$$

$$\mathrm{PI{-}P(S{-}I)_tPS^-Li^+} + \mathrm{MeOH} \rightarrow \mathrm{PI{-}P(S{-}I)_t{-}PS}$$

Three triblock copolymers were synthesized with an inverse tapered middle block (ITMB) (T1, T2, T3). The only difference between the synthesis of ITMB and TMB is the inversion of the order of addition of the monomers. Using this procedure, the I-rich part of the middle block is close to the PS block and the S-rich part close to the PI block. The different steps of the procedure followed are given below:

$$\mathrm{S} + s\text{-BuLi} \rightarrow \mathrm{PS^-Li^+}$$

$$\mathrm{PS^-Li^+} + \mathrm{S} + \mathrm{I} \rightarrow \mathrm{PS{-}P(S{-}I)_{inv.t}^-\,Li^+}$$

$$\mathrm{PS{-}P(S{-}I)_{inv,t}^-Li^+} + \mathrm{I} \rightarrow \mathrm{PS{-}P(S{-}I)_{inv,t}{-}PI^-Li^+}$$

A random copolymer (R1) was synthesized using the potassium alkoxide of 2,3-dimethyl-3-pentanol. It was concluded that a 30/1 ratio of Li/K was optimal in order to produce copolymers with random composition:[11−14]

$$s\text{-BuLi} + \mathrm{S} + \mathrm{I} + \text{potassium alkoxide} \rightarrow \mathrm{P(S{-}I)_r^-Li^+}$$

$$\mathrm{P(S{-}I)_rLi^+} + \mathrm{MeOH} \rightarrow \mathrm{P(S{-}I)_r}$$

Two normal diblock copolymers (D1 and D2) were also synthesized by sequential addition of S and I to a *s*-BuLi solution in benzene, for comparison reasons. A schematic drawing of the block copolymer architectures synthesized is given in Figure 1.

Molecular Characterization. All samples were characterized by a variety of methods. Intermediate and final products were analyzed by size exclusion chromatography, using RI and UV detection, in terms of sample homogeneity and molecular weight distributions, in tetrahydrofuran (THF). SEC analysis was performed at 308 K with a Waters system equipped with a Waters 501 HPLC pump, Waters Styragel columns having a porosity range of 10^3−10^5 Å, a Waters 410 differential refractometer, and a Waters 486 tunable UV detector. Calibration curves were prepared with polystyrene standards.

Number-average molecular weights (M_n) of each part of the molecules were obtained by membrane osmometry (MO) at 310 K in toluene with a Jupiter Instrument Co. model 231 membrane osmometer. RC-51 membranes were used with toluene distilled over CaH_2 as the solvent. The average composition of the samples was determined by ^{1}H NMR spectroscopy (Bruker AC200 instrument) in $CDCl_3$ at 303 K. The targeted composition of the copolymers synthesized was 50 vol % in either components. The molecular characteristics of the polymers are given in Table 1. Dielectric spectroscopy on the final products and their block copolymer precursors indicated a blocky structure within the interface with some mixing of segments in the center of the midblock. The dielectric spectroscopy results on the segmental and end-to-end vector dynamics support the composition variation shown in Figure 1 and will be discussed elsewhere in detail.[15]

Transmission Electron Microscopy (TEM). A Zeiss EM 902 electron microscope operated at 80 kV using an objective aperture of 8 mrad was used. The samples were used in the melt state and were annealed for 1 day at temperatures corresponding to the PS glass transition. Prior to sectioning, at 243 K, all samples were exposed to OsO_4 vapor for 8 h. Ultrathin sections were produced using a Reichert ultramicrotome with FC4 cryo attachment at 218 K. Sections were floated off the knife onto aqueous dimethyl sulfoxide solution. Following sectioning all samples were again exposed to OsO_4 vapor for additional 16 h. Micrographs were recorded on a Kodak FGRP 35 mm film. Figure 2 provides four TEM images of the copolymers T1, T2, T3, and T4. The dark and bright phases correspond to PI- and PS-rich domains, respectively.

Differential Scanning Calorimetry (DSC). A Polymer-Laboratories DSC was used with an integral cooling jacket capable of programmed cyclic temperature tests over the range 113−673 K. A dry gas purge was used for accurate measurements near ambient temperature ranges. Two cooling and subsequent heating runs have been performed within the T limits 200−448 K and with rates of 20 and 10 K/min. The glass transitions obtained from the second run (10 K/min) are shown in Table 2.

Small-Angle X-ray Scattering (SAXS). A Kratky compact camera (Anton Paar KG) equipped with a one-dimensional position-sensitive detector (M. Braun) was used for the SAXS experiment. The Ni-filtered Cu Kα radiation ($\lambda = 0.154$ nm) was used from a Siemens generator operating at 35 kV and

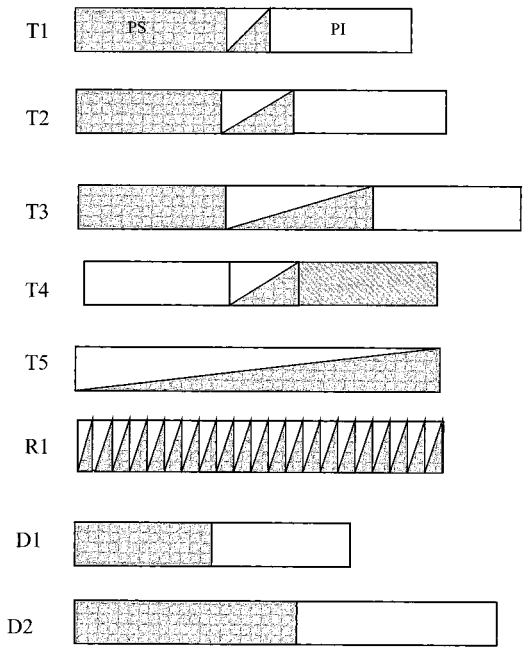

Figure 1. Schematic of the inverse taper (T1, T2, T3), the normal taper (T4, T5) block copolymers, the random block copolymer (R1), and the diblock copolymers (D1, D2). The gray and white areas indicate polystyrene and polyisoprene regions, respectively.

30 mA. Measurements of 1 h long were made at intervals of 5 K within the range 303−433 K and up to 493 K for T4, and the stability was better than ±0.2 K. Changes between successive temperatures were completed within ~5 min, and a 30 min waiting time was preset for equilibration. The smeared intensity data were collected in a multichannel analyzer and transferred to a computer for further analysis. Smeared intensities were subsequently corrected for absorption, background scattering, and slit-length smearing. Primary beam intensities were determined, in absolute units, by using the moving slit method.

Rheology. An advanced rheometric expansion system (ARES) equipped with a force-rebalanced transducer was used in the oscillatory mode. Different types of experiments have been performed. First, the linear and nonlinear viscoelastic ranges were identified by recording the strain amplitude dependence of the complex shear modulus G^*. In all the experiments strain amplitudes within the linear viscoelastic range were used. These experiments involved (i) isochronal temperature scans within the range 303−473 K, at 1 rad/s, aiming to identify the order-to-disorder transition temperatures, and (ii) isothermal frequency scans for temperatures in the range 303−473K and for frequencies $10^{-2} < \omega < 10^2$ rad/s.

III. Results and Discussion

All the copolymers studied had a nearly symmetric composition (Table 1); therefore, the expected morphology is lamellar. SAXS and TEM have shown that this is indeed the case for all copolymers except for the inverse tapered block copolymer T3 and the all-tapered block copolymer T5, for which a homogeneous (disordered) phase is found at 303 K. The TEM images depicted in Figure 2 show lamellar structures in the inverse tapered copolymers T1 and T2 as well as in the normal tapered copolymer T4. Some typical spacings can be calculated from the images shown which correspond to distances of about 14 nm in T1 and T2 and to 18.5 nm in T4. These spacings are only indicative for the characteristic distances and are actually smaller (due to inclination of the lamellar planes) from the corresponding values obtained in SAXS (see below). Nevertheless, the TEM images show a longer characteristic spacing in the normal tapered copolymer T4, despite its similar molecular weight with the inverse tapered copolymer T2.

The SAXS spectra revealed also that the inverse tapered block copolymer T3 with the broader interface forms a disordered phase at 303 K in contrast to the T1, T2, and T4 copolymers which have a lamellar microstructure with respective order-to-disorder transition temperatures of 388, 366, and 460 K (Table 2). The all-tapered block copolymer T5 exhibits a disordered phase with a liquidlike structure factor, whereas the random copolymer R1 shows only a decaying intensity with increasing wavevector which is expected from the random block structure (disordered) and the absence of a well-defined distance. As representative of the structural changes occurring at the ODT we show the SAXS spectra for the inverse tapered block copolymer T1 in Figure 3. The intense peak of the structure factor below the ODT, originating from the correlations between the PS and PI domains forming the lamellar, "melts" at the T_{ODT}, leaving a broad liquidlike structure factor in the disordered phase originating from the weaker correlations due to the block connectivity.

The changes in the SAXS spectral shape for the different copolymers are better depicted in Figure 4 where the main peak parameters (inverse peak intensity, width, and position) are plotted as a function of inverse temperature. All peak parameters for the T1 and T2 and to a lesser extent for the T4 copolymer are discontinuous at their respective ODT, and this is in contrast to the continuous changes observed for the T3 and T5 block copolymers, which remain in the disordered phase at all temperatures investigated. The discontinuous changes of the peak parameters provide the means for a qualitative identification of the T_{ODT} in the tapered block copolymers. Here we mention, parenthetically, that the transition is accompanied by a small enthalpy of fusion (about 1 J/g) as shown by DSC, which is indicative of a first-order transition.[16,17] According to the predictions of the mean-field theory,[18] the T dependence of the peak intensity should follow from

$$\frac{N}{S(Q)} = F(x,f) - 2\chi N \qquad (1)$$

where $S(Q)$ is the static structure factor, $x = (QR_g)^2$, and $F(x,f)$ is a term containing combinations of Debye functions that depend strongly on the molecular architecture. Given that in the simplest approximation χ is inversely proportional to temperature, a plot of $S(Q^*)^{-1}$ vs T^{-1} in the disordered phase should yield a linear dependence. However, the $I(Q^*)^{-1}$ vs T^{-1} data shown in Figure 4 display curvature, and this has been discussed in terms of fluctuation corrections which alter the $S(Q)$ as[19]

$$\frac{N}{S(Q)} = F(x,f) - 2\chi N + \frac{c^3 d\lambda}{\bar{N}^{1/2}}\sqrt{\frac{S(Q^*)}{N}} \qquad (2)$$

where $\bar{N} = Na^6/u^2$ (a and u are the statistical segment length and volume, respectively) is a Ginzburg parameter, and c and λ are composition-dependent coefficients and $d = 3x^*/2\pi$. Equation 2 correctly predicts that

Table 1. Molecular Characteristics of the Block Copolymers

sample	$M_{n,PS}{}^a \times 10^{-3}$	$M_{n,P(S/I)}{}^b \times 10^{-3}$	$M_{n,PI}{}^b \times 10^{-3}$	$M_n$total$^b \times 10^{-3}$	$M_w/M_n{}^a$	$w_{PS}{}^c$ %	$N^*_{n,PS}{}^d$	$N^*_{n,PI}{}^d$	$f_{PS}{}^e$
T1:PS−P(I/S)−PI	8.6	2.0	7.9	18.5	1.02	50.8	103	117	0.47
T2:PS−P(I/S)−PI	7.8	5.2	9.8	22.8	1.03	51.4	129	143	0.47
T3:PS−P(I/S)−PI	8.5	8.7	9.2	26.4	1.03	51.8	150	164	0.48
T4:PS−P(S/I)−PI	9.5	5.5	7.8	22.8	1.02	56.8	142	127	0.53
T5:P(S/I)t		23.1		23.1	1.03	51.9	132	143	0.48
R1:P(S/I)r		24.3		24.3	1.03	53.6	143	145	0.49
D1:PS−PI	8.0		8.7	16.7	1.03	49.8	91	108	0.46
D2:PS−PI	12.4		17.2	29.6	1.04	50.9	166	187	0.47

[a] By size exclusion chromatography (SEC) in THF at 35 °C. [b] By membrane osmometry in toluene at 37 °C. [c] By ^{1}H NMR spectroscopy in $CDCl_3$ at 30 °C. [d] $N^*_{n,PS} = N_{n,PS}(\rho^*_I/\rho^*_S)^{1/2}$ and $N^*_{n,PI} = N_{n,PI}(\rho^*_S/\rho^*_I)^{1/2}$. [e] $f_{PS} = N^*_{n,PS}/(N^*_{n,PS} + N^*_{n,PI})$.

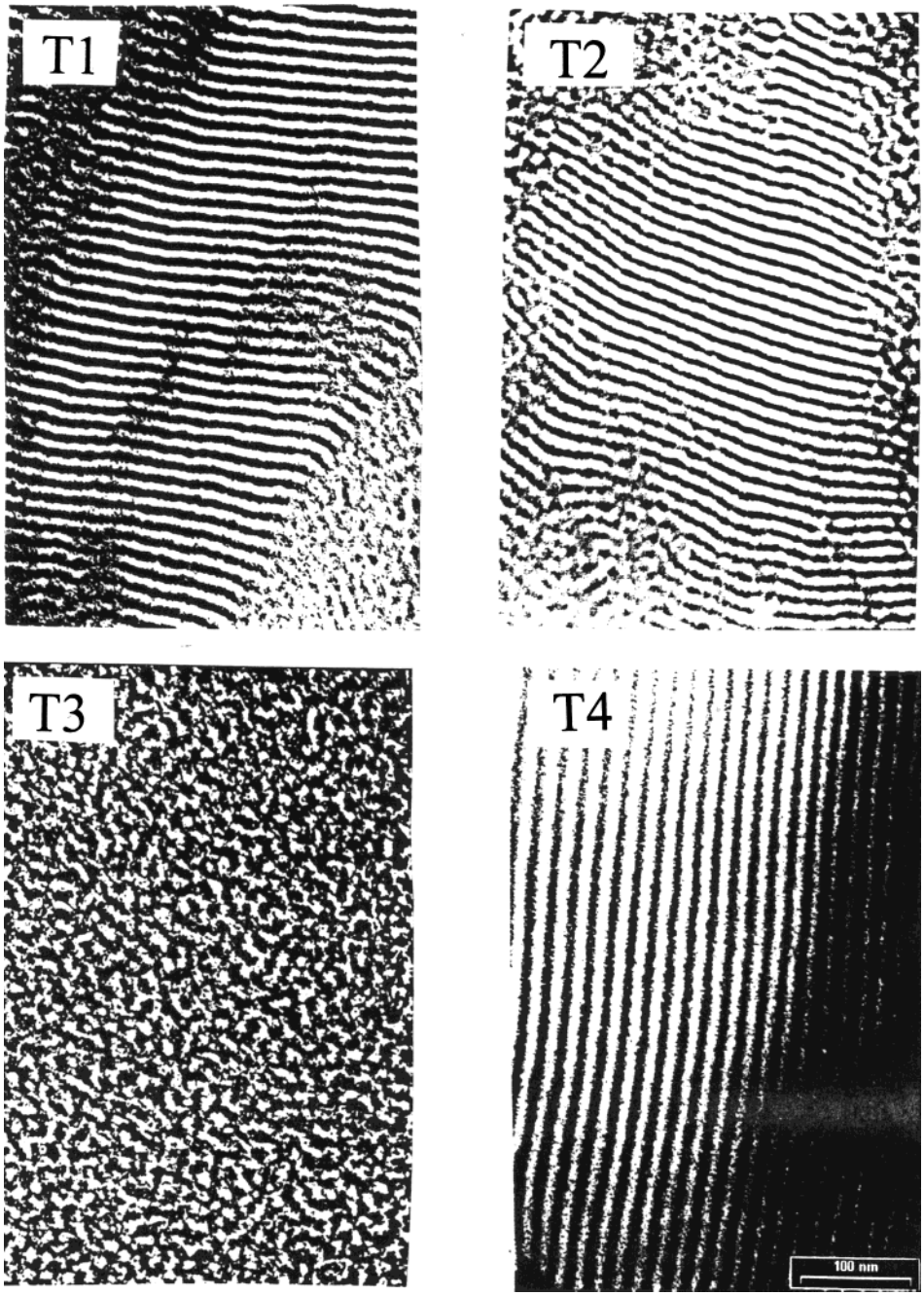

Figure 2. Microdomain structure of the block copolymers observed by transmission electron microscopy on sections stained by OsO_4. A lamellar structure is formed in the inverse tapered block copolymers T1 and T2 and the normal tapered block copolymer T4, whereas in T3 a disordered structure is found.

$S(Q^*)^{-1}$ has a nonlinear dependence on T^{-1}. However, a one-to-one comparison with the experimental data requires copolymers of very high molecular weights since the approximations leading to eq 2 are only accurate for very high values of N. In short, the quantitative identification of the T_{ODT} from the SAXS spectra revealed that the transition temperature decreases in going from T1 to T2 to T3 block copolymers,

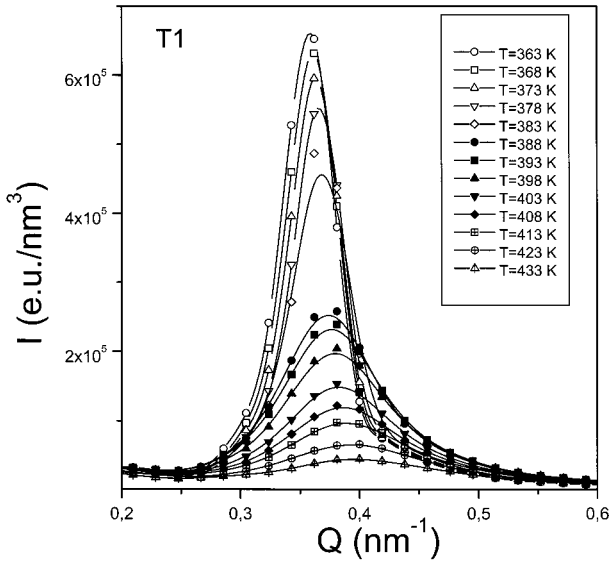

Figure 3. Representative SAXS profiles of the inverse tapered copolymer T1 at different temperatures as indicated. The order-to-disorder transition temperature is at 388 K.

Table 2. Transition Temperatures of the Tapered Copolymers (T1, T2, T3, T4, and T5), the Random Copolymer (R1), the Diblocks (D1 and D2), and the Blends of the Diblocks (D1/D2)$_\alpha$ and (D1/D2)$_\beta$

sample	T_g (K) (PI/PS)	T_{ODT} (K)	$(\chi N)_c$
T1	210/373	388	10.5
T2	211/368	366	14.7
T3	213/363	$<T_g^{PS}$	>19.5
T4	211/373	460	8.6
T5	220/323	$<T_g^{PS}$	>17
R1	~300	homogeneous	
D1	210/373	373	10.4
D2	210/373	476	10.3
(D1/D2)$_\alpha$		378	11.2
(D1/D2)$_\beta$		407	11.8

i.e., with increasing interfacial width, however, it increases in the normal tapered copolymer T4.

Rheology is also employed as a probe of the viscoelastic changes occurring at temperatures above the PS glass transition. Some representative results are shown in Figures 5 and 6 for the inverse tapered copolymer T1 and the normal tapered copolymer T4. The frequency dependence of the storage and loss moduli shown in Figure 5 for T1 nicely display the effects of the PS glass transition and of the ODT on the viscoelastic properties of these complex materials. The $G'(\omega)$ and $G''(\omega)$ spectra obtained during the isothermal frequency scans were subsequently shifted to the corresponding spectrum at 313 K. Strictly speaking, the use of time−temperature−superposition (tTs) is not valid in systems with a T-dependent internal structure such as block copolymers. Nevertheless, we still show the result of the attempted tTs to illustrate how the different processes affect the viscoelastic response of the system. Starting from higher frequencies, the spectra for the storage and loss moduli are influenced by (i) the PS segmental relaxation, (ii) the PS block relaxation, and at lower frequencies by (iii) the microdomain relaxation. The latter process usually appears as an extrapolation of process ii to lower frequencies.[20−22] At low frequencies and for temperatures above the ODT the viscoleastic response of the system becomes fluidlike (terminal) with slopes of 1 and 2 for the loss and storage moduli, respectively. Another way of determining the ODT,

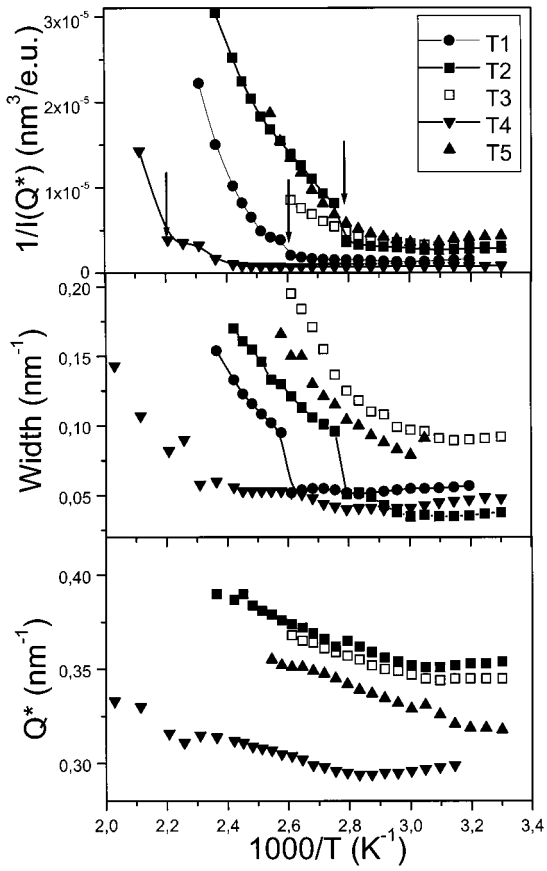

Figure 4. Comparison of the peak parameters (inverse peak intensity, peak position, and width) for the inverse tapered copolymers: T1 (●), T2 (■), T3 (□), the regular tapered copolymer T4 (▼), and the all-tapered copolymer T5 (▲). Arrows indicate the transition temperatures for T1, T2, and T4.

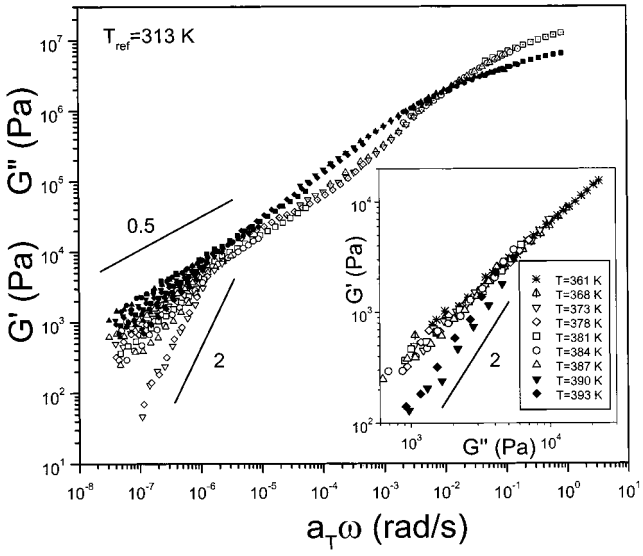

Figure 5. Reduced frequency plots for the storage (open symbols) and loss (filled symbols) moduli of the inverse tapered block copolymer T1. The reference temperature was 313 K, and the strain amplitude was below 4%. Two lines with slopes of 0.5 and 2 are shown. The ODT obtained from this reduced frequency representation is at 390 K. In the inset the data are plotted in the $G'-G''$ representation and show that the ODT is again at 390 K.

which does not require the use of tTs, is by plotting the logarithm of the storage moduli as a function of the logarithm of the loss moduli for the different tempera-

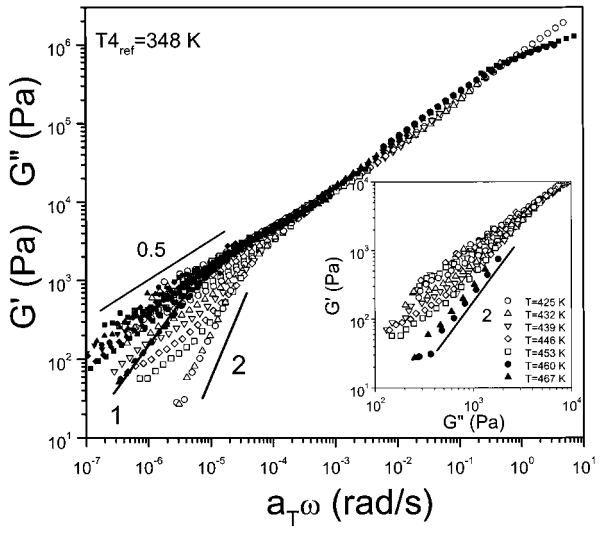

Figure 6. Reduced frequency plots for the storage (open symbols) and loss (filled symbols) moduli of the regular tapered block copolymer T4. The reference temperature was 348 K, and the strain amplitude was below 4%. Two lines with limiting slopes at low frequencies are shown (2 and 1 for the loss and storage moduli, respectively). The ODT obtained from this reduced frequency representation is at 460 K. In the inset the data are plotted in the $G'-G''$ representation and show that the ODT is also at 460 K.

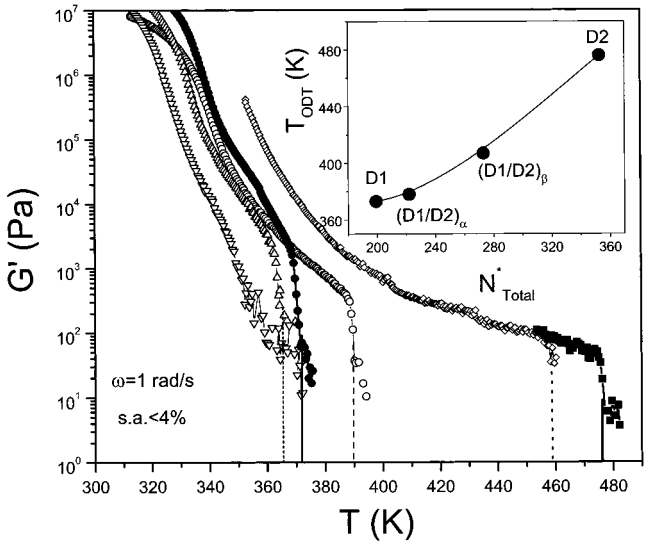

Figure 7. Isochronal measurements of the storage modulus of the inverse tapered copolymers T1 (○), T2 (△), and T3 (▽), the normal tapered copolymer T4 (◇), and the two diblock copolymers D1 (●) and D2 (■). All measurements were made at a frequency of 1 rad/s and with a strain amplitude below 4%. In the inset, the T_{ODT} is plotted as a function on N^*_{total} for the pure diblocks D1 and D2 and their mixtures, $(D1/D2)_\alpha$ and $(D1/D2)_\beta$.

tures (known as the Han representation).[23] In this representation, and for symmetric copolymers, the ODT corresponds to a temperature where the slope attains a value of 2. Again, the two representations give identical results for the transition temperature ($T_{ODT} \approx 390$ K). Similar results have been obtained for the other inverse tapered copolymers, and the results for the transition temperatures are summarized in Table 2.

The corresponding viscoelastic processes for the normal tapered block copolymer T4 are shown in the shifted data of Figure 6. Again, the two representations used in Figure 5 yield equivalent results for the transition temperature ($T_{ODT} = 454$ K). There is, however, a significant difference between the results shown for the tapered block copolymers and the normal diblock copolymers D1 and D2 as well as for other diblocks of similar molecular weights investigated so far.[22,24] The spectra of Figures 5 and 6 show that the viscoelastic response of the tapered and inverse tapered copolymers at temperatures below the ODT exhibit a T dependence with many intermediate states which fail to superimpose. It appears that the existence of the tapered interface increases the contribution of fluctuations.

The rheological results from all the copolymers are summarized in Figure 7 where the isochronal temperature scans from the normal tapered, the inverse tapered, and the pure diblocks are compared at 1 rad/s and for low strain amplitude (below 4%). The T-dependent storage moduli exhibit the three processes discussed before with respect to the frequency dependence and show the ODT from the discontinuous drop of the moduli at the corresponding temperatures. Notice that for the inverse tapered copolymer T3 a continuous change is observed instead. For this copolymer, the ODT is in the proximity of the PS glass transition which inhibits the formation of a mesophase, and this is in good agreement with the results from SAXS (Figure 4) and TEM (Figure 2). The corresponding data and the transition temperatures for the two diblock copolymers D1 and D2 are also shown in Figure 7 (with the solid symbols) for comparison.

The SAXS, TEM, and rheological studies have shown that (i) increasing the gradient interface results in a decrease of the T_{ODT} (T3 vs T2 and T1) and that (ii) the degree of segregation depends strongly on the type of tapered copolymer; i.e., normal vs inverse tapered copolymers of the same molecular weights have completely different transition temperatures (T2 vs T4). One way to account for the decrease of the ODT with the increase of the tapered midblock in the inverse tapered copolymers is to compare their transition temperatures with normal diblocks of identical molecular weight and composition. The synthesis of such new diblock copolymers that meet these requirements is at least time-consuming so a different method was employed: we have prepared the required diblocks by mixing the existing D1 and D2 in different ratios: $(D1/D2)_{\alpha-}$ and $(D1/D2)_{\beta-}$ that would correspond to the molecular weights of the T1 and T2 inversed tapered copolymers. The (single) measured T_{ODT} for each of the "new" diblocks is plotted in the inset to Figure 7 in comparison to the normal diblocks D1 and D2 and are also shown in Table 2. For the $(D1/D2)_{\alpha-}$ mixture, the ODT is in the vicinity of the inverse tapered T1 which indicates that about 20% of segments within the interface might be the norm in regular diblock copolymers.[25] On the other hand, in the T2 inverse tapered copolymer, the ODT is reduced by as much as 41 K with respect to the $(D1/D2)_{\beta-}$ mixture, indicating that increasing the amount of the tapered midblock results in a more compatible system. It is therefore not surprising that in the T3 the ODT is depressed so that the copolymer remains practically in the disordered phase.

Another way of discussing the increased compatibility in the inverse tapered copolymers as well as the opposing effect in the normal tapered copolymer is by calculating the shift in the spinodals for the given copolymer compositions. This type of representation requires knowledge of the $\chi(T)$. Here, as a first ap-

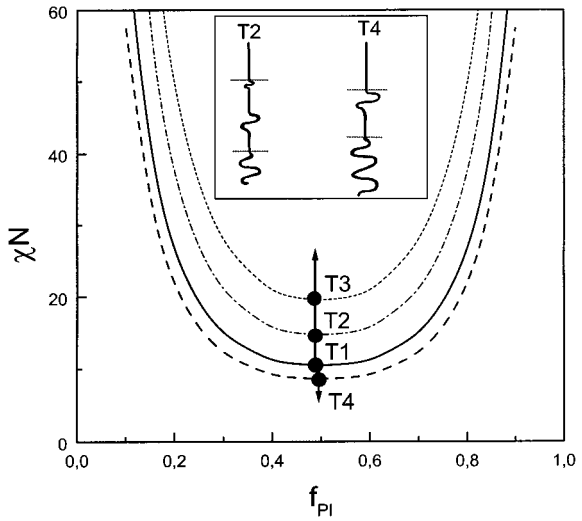

Figure 8. Schematic phase diagram showing the location (spinodals) of the inverse and normal tapered copolymers. Notice that increasing the molecular weight of the midblock in the inverse tapered copolymers (T1, T2, T3) increases the compatibility whereas the opposite is happening in the normal tapered copolymer T4. In the inset, the structures of T2 and T4 are compared. Notice the smaller effective interfacial width in the latter.

proximation, we have assumed that $\chi(T)$ will remain unchanged by the PS and PI segments at the tapered interface; i.e., correlations between the segments will be unchanged by the presence of the interface. This is certainly a very rough approximation. On the basis of a binary interaction theory,[26] the effective interaction parameter (χ_{eff}) will be reduced relative to the pure diblock case (χ); if f_{SS} and f_{IS} are respectively the volume fractions of styrene in the styrene-rich and isoprene-rich blocks, then $\chi_{eff} = \chi(f_{SS} - f_{IS})^2$. This reduction in the effective interaction parameter is expected to lower the T_{ODT} considerably. Within our approximation, however, for the $\chi(T)$ determination we have used the MFT prediction, i.e., $(\chi N)_c = 10.5$ for the two diblock copolymers D1 and D2. This procedure results in the following T dependence: $\chi(T) = 40/T - 0.005$ (fluctuation corrections result in a stronger dependence, i.e., $\chi = 62/T - 0.09$) and allows, within our approximation, a direct comparison of the spinodals for each of the copolymers investigated. The result is depicted in Figure 8. As shown in the figure, increasing the interface in the inverse tapered block copolymers results in an increasing compatibility. The effect is significant; in going form T1 to T2 the critical value of χN increases from 10.5 to 14.7. We mention here that a grafted copolymer of the AB_2 type increases the intrinsic compatibility relative to the linear AB diblock by shifting the spinodal to 13.5,[27] and increasing the number of B-blocks to three or even higher (i.e., in AB_3 or AB_4) does not increase this value (in fact, it decreases the critical value).[28] Therefore, the effect of varying the interfacial width in the inverse tapered copolymers is significant and suggests a new way of increasing block compatibility. The effect of the sequencing of the blocks with respect to the interface is also significant. The normal tapered copolymer T4, with a similar number of segments within the PS and PI blocks as well as in the interface, is much more *incompatible* than the T2. This is shown in the SAXS data of Figure 4 and the rheology data of Figures 6 and 7 with the increase of the T_{ODT} by about 100 K relative to T2 and by the lower $(\chi N)_c$ value of about 8.6.

The explanation for the drastically different compatibility of T2 and T4 can be found in the opposite block sequencing in the tapered interface. In the inverse tapered copolymer T2, next to the long outer blocks of PS and PI there are always short blocks of the *opposite* kind. On the other hand, in the normal tapered copolymer T4, next to the PS and PI outer blocks there are long blocks of the *same* kind. Consequently, the effective interfacial width is reduced in T4 relative to T2, and the system becomes more incompatible. This situation is depicted schematically in the inset to Figure 8. The higher incompatibility in T4 is in agreement with the reduced Q^* relative to T2 (Figure 4). At 357 K, the long spacings of T2 and T4 are 17.2 and 21.2 nm, respectively. The higher domain spacing in the latter implies higher chain stretching and thus increased incompatibility which drives the system toward stronger segregation. On the basis of the known volume fractions, we calculate the following PS and PI effective domain spacings: 8.1 and 9.1 nm in T2 and 11.2 and 10 nm in T4, which implies an effective extension of 3 and 1 nm, respectively, for the PS and PI domains in T4.

Herein, we have investigated the effect of a composition gradient along the interface in symmetric block copolymers of styrene and isoprene. The corresponding alteration in the dynamics will be discussed next.[15] In the future it would be of interest to study also asymmetric tapered block copolymers with respect to morphological changes which can be triggered by block sequencing in normal and inverse tapered copolymers.

IV. Conclusion

The systematic variation of the amount of interfacial material as well as the effect of block sequencing in tapered and inverse tapered block copolymers allowed the following conclusions to be made:

1. Tapered and inverse tapered block copolymers exhibit first-order transitions at the order-to-disorder transition temperature as evidenced by the existence of a latent heat in calorimetry and from the discontinuous changes of the structure factor and the viscoelastic properties.

2. All copolymers formed the typical microdomain structure expected from their nearly symmetric composition (lamellar).

3. An inverse tapered copolymer with about 20% of the segments within the tapered interface was found to have the same ODT with a diblock copolymer of similar molecular weight. This may indicate that normal diblock copolymers of such molecular weights have considerable interfacial mixing.

4. The increase of the amount of material within the tapered interface was found to enhance the compatibility in a systematic way.

5. Block sequencing in the tapered interface with respect to the outer blocks is the most important factor controlling compatibility. Inverse tapered block copolymers are much more compatible than the corresponding normal tapered copolymers.

The results presented above provide the means of designing new block copolymers with a highly controlled compatibility at the synthesis level, which can be triggered by two independent parameters: the block sequencing *and* the amount of tapered midblock.

Acknowledgment. This work was supported by the TMR network CAPS (No. FMRX-CT97-0122). We ac-

knowledge our partners of the CAPS network for discussions. We are grateful to Dr. G. Lieser at the Max-Planck-Institute for Polymer Research in Mainz for the TEM study as well as to Prof. T. Pakula for illuminating discussions.

References and Notes

(1) Zelinski, R.; Childers, C. W. *Rubber Chem. Technol.* **1968**, *41*, 161.
(2) Knoll, K.; Niessner, N. *Macromol. Symp.* **1998**, *132*, 231.
(3) Anmghoefer, F.; Gronski, W. *Colloid Polym. Sci.* **1983**, *261*, 15.
(4) Tsukahara, Y.; Nakamura, N.; Hashimoto, T.; Kawai, H. *Polym. J.* **1980**, *12*, 455.
(5) Hashimoto, T.; Tsukahara, Y.; Kawai, H. *Polym. J.* **1983**, *10*, 699.
(6) Hashimoto, T.; Tsukahara, Y.; Tachi, K.; Kawai, H. *Macromolecules* **1983**, *16*, 648.
(7) Pakula, T.; Matyjaszewski, K. *Macromol. Theory Simul.* **1996**, *5*, 987.
(8) Morton, M.; Fetters, L. J. *Rubber Chem. Technol.* **1975**, *48*, 359.
(9) Roovers, J.; Toporowski, P. *Macromolecules* **1983**, *16*, 843.
(10) Young, R. N.; Quirk, R. P.; Fetters, L. J. *Adv. Polym. Sci.* **1984**, *56*, 1.
(11) Smith, S. D.; Ashraf, A. *Polym. Prepr.* **1993**, *34* (2), 672.
(12) Ashraf, A.; Smith, S. D.; Spontak, R. J.; Clarson, S. J.; Lipscomb, G.; Satkowski, M. M. *Polym. Prepr.* **1994**, *35 (1)*, 581.
(13) Hsieh, H. L.; Wofford C. F. *J. Polym. Sci.* **1969**, *7*, 449.
(14) Wofford, C. F.; Hsieh, H. L. *J. Polym. Sci.* **1970**, *7*, 461.
(15) Hodrokoukes, P.; Floudas, G.; Pispas, S.; Hadjicristidis, N. Manuscript in preparation.
(16) Floudas, G.; Hadjicristidis, N.; Stamm, M.; Likhtman, A. E.; Semenov, A. N. *J. Chem. Phys.* **1997**, *106*, 3318.
(17) Hajduk, D. A.; Gruner, S. M.; Erramilli, S.; Register, R. A.; Fetters, L. J. *Macromolecules* **1996**, *29*, 1473.
(18) Leibler, L. *Macromolecules* **1980**, *13*, 1602.
(19) Fredrickson, G. H.; Helfand, E. *J. Chem. Phys.* **1987**, *87*, 697.
(20) Rosedale, J. H.; Bates, F. S. *Macromolecules* **1990**, *23*, 2329.
(21) Floudas, G.; Hadjichristidis, N.; Iatrou, H.; Pakula, T.; Fischer, E. W. *Macromolecules* **1994**, *27*, 7735.
(22) Floudas, G.; Pispas, S.; Hadjichristidis, N.; Pakula, T.; Erukhimovich, I. *Macromolecules* **1996**, *29*, 4142.
(23) Han, C. D.; Baek, D. M.; Kim, J. K.; Ogawa, T.; Sakamoto, N.; Hashimoto, T. *Macromolecules* **1995**, *28*, 5043.
(24) Floudas, G.; Pakula, T.; Fischer, E. W.; Hadjichristidis, N. Pispas, S. *Acta Polym.* **1994**, *45*, 176.
(25) Schubert, D. W.; Pannek, M.; Muller, A. H. E. *Physica B* **2000**, *276−278*, 365.
(26) Roe, R.-J.; Zin, W. C. *Macromolecules* **1980**, *13*, 1221. Ten Brinke, G.; Karasz, F. E.; MacKnight, W. J. *Macromolecules* **1983**, *16*, 1827. Paul, D. R.; Barlow, J. W. *Polymer* **1984**, *25*, 487.
(27) Olvera de la Cruz, M.; Sanchez, I. C. *Macromolecules* **1986**, *19*, 2501.
(28) Floudas, G.; Hadjichristidis, N.; Tselikas, Y.; Erukhimovich, I. *Macromolecules* **1997**, *30*, 3090.

MA001479I